Wu et al. Sustainable Chemical Processes 2014, 2:5
http://www.sustainablechemicalprocesses.com/content/2/1/5

SUSTAINABLE CHEMICAL PROCESSES

RESEARCH ARTICLE Open Access

Scenario analysis of a bioethanol fueled hybrid power generation system

Wei Wu[1*], Yuan-Tai Hsu[2] and Po Chih Kuo[1]

Abstract

Background: Regarding most of FC/PV/Battery based hybrid power generation systems, the photovoltaic (PV) power usually dominates the main power supply and the water electrolyzer is used to produce hydrogen. The energy efficiencies of these hybrid power generation (HPG) systems are usually low due to the low conversion efficiency of PV cell and the extra power consumption to hydrogen production. To reduce the electricity demand by the PV system and improve the energy efficiency of hydrogen production unit, a scenario-based design of the HPG system is necessary.

Result: This paper proposes an EFC/PV/Battery based hybrid power generation system to meet 24-hour power demand. An ethanol-fueled fuel cell (EFC) power generator not only dominates the main power supply, but also a combination of the stand-alone EtOH-to-H2 processor and PEMFC can ensure higher energy efficiency. A PV system is treated as an auxiliary power generator which can reduce the (bio)ethanol consumption. A backup battery not only stores excess power from PV or EFC, but also it can precisely satisfy the power demand gap. Finally, scenario analysis of the hybrid power generation (HPG) system in regard to the hybrid power dispatch and energy efficiency is addressed.

Conclusion: An optimized fuel processing unit using ethanol fuel can produce high-purity hydrogen. The simulation shows that the stand-alone EtOH-to-H2 processor not only guarantee the high energy efficiency, but also it can continuously produce hydrogen if the fuel is enough. According to scenarios for the daily operation of the HPG system, the EFC power dominates the power supply during the night, the PV system dominates the power supply during the day and the backup battery aims to instantly compensate the power gap and store the excess power from PV or EFC. According to the hybrid power dispatch, the distribution of the HPG system efficiency is specified.

Keywords: Hybrid power system, Scenario analysis, Ethanol-fueled fuel cell system, Energy efficiency

Background

Recently the interest in renewable and sustainable power generation techniques such as photovoltaic, wind, and fuel cell powered systems has grown. The off-grid hybrid power system is increasingly popular for remote area power generations, even though the photovoltaic (PV) or wind system is highly dependent on weather conditions and locations. Muselli et al. [1] developed a stand-alone hybrid power system which was composed of the PV panels, an electrical generator using fossil fuels, and battery storage, and Elhadidy [2] studied the feasibility of using wind/solar/diesel energy conversion systems to meet the power demand of the specific community in Saudi Arabia. Notably, a gasoline or diesel engine is usually treated as the backup power generator.

The PV system generates electricity during daylight hours, but the fuel cell system produces electricity as long as hydrogen is supplied. To address the clean power generation system, Hwang et al. [3] proposed a solar/fuel cell hybrid power system to meet the daily load demand of a typical family in Taiwan, Uzunoglu et al. [4] investigated dynamic models and simulation of this kind of hybrid power generation systems with appropriate control strategies, and Zervas et al. [5] provided an optimal decision framework for managing the hybrid energy systems. Similarly, these hybrid systems all involve the water

* Correspondence: weiwu@mail.ncku.edu.tw
[1]Department of Chemical Engineering, National Cheng Kung University, Tainan 70101, Taiwan
Full list of author information is available at the end of the article

electrolyzer for producing hydrogen. The electrolyzer is simpler and does not require complex units, but there is no solution to reduce its large electricity consumption. For most of hybrid systems, the PV panel is larger so as to carry out water electrolysis by using the excess power. Therefore, the overall energy efficiency is quite low [6].

The hydrogen fuel cells have been considered the most promising for automotive application, but the guidelines for the hydrogen storage, safer operation and transportation are quite rigorous [7]. The fossil fuel processing unit could produce the high purity of hydrogen [8,9], but the external energy supply and large carbon emissions are not avoided. If biomass can replace fossil fuels as the feedstock, the net-zero greenhouse gas (GHG) emissions of hydrogen production systems can be achieved. Liquefied ethanol is a popular feedstock because it is easily made by fermentation, no compressed storage is needed, and lower operating temperatures are required for reforming processes [10,11].

In this paper, an ethanol fueled HPG system is proposed. The modeling, optimization and design of the EtOH-to-H_2 processor is achieved by using Aspen Plus. The scenario analysis of the HPG system in regard to the daily load demand of a typical family in Taiwan [3] is investigated in Matlab. Since the EFC power unit cannot rapidly meet the load demand due to complicated chemical reactions in the ethanol reforming process, the lithium-ion battery is considered to meet the power gap when the excess power from PEMFC and PV units have been completely stored in the battery in advance. According to prescribed hybrid power dispatch, it is verified that the energy efficiency of the proposed HPG system is superior to the other renewable hybrid energy system.

Hybrid power generation system

The ethanol-fueled HPG system is shown in Figure 1. Both PV generator and PEMFC stack are treated as power sources. The lithium-ion battery is denoted as an electricity storage/instant supply device. The stand-alone EtOH-to-H_2 processor in place of the devices of the hydrogen storage tank and water electrolyzer aims to produce high purity hydrogen. Other devices, including converters/inverters and power management (DC bus), are used to meet the voltage specification.

EtOH-to-H_2 processor

The EtOH-to-H_2 processor shown in Figure 2 is considered as a stand-alone hydrogen production system, which is composed of an ethanol steam reforming (ESR) reactor, a low-temperature water-gas-shift (LTWGS) reactor, the pressure swing adsorption (PSA) unit, and a burner. The simple heat integration is adopted to improve the water heat recovery; (i) the waste heat generated from the burner is applied to preheat the mixing feed flow using a heat exchanger (HEX1) and then meets the heat demand of the reforming reactions in the ESR reactor; (ii) the inlet water flow is preheated by a heat exchanger (HEX2) to increase the feed temperature; (iii) the temperature of flue gas discharged from the heating jacket of the ESR reactor is expected to be low.

ESR reactor

According to the kinetic experiments for the ethanol steam reforming reactions over Co_3O_4-ZnO catalyst at atmospheric pressure and temperature in the 600-800 K range [12], first the reactions of ESR are shown as:

$$C_2H_5OH \rightarrow CH_3CHO + H_2\ (r_1), \Delta H_1^0 = 71\ \text{kJ mol}^{-1} \quad (1)$$

$$C_2H_5OH \rightarrow CO + CH_4 + H_2\ (r_2), \Delta H_2^0 = 52.9\ \text{kJ mol}^{-1} \quad (2)$$

$$CO + H_2O \leftrightarrow CO_2 + H_2\ (r_3), \Delta H_3^0 = -34.5\ \text{kJ mol}^{-1} \quad (3)$$

$$CH_3CHO + 3H_2O \rightarrow 2CO_2 + 5H_2\ (r_4), \Delta H_4^0 = 127.4\ \text{kJ mol}^{-1} \quad (4)$$

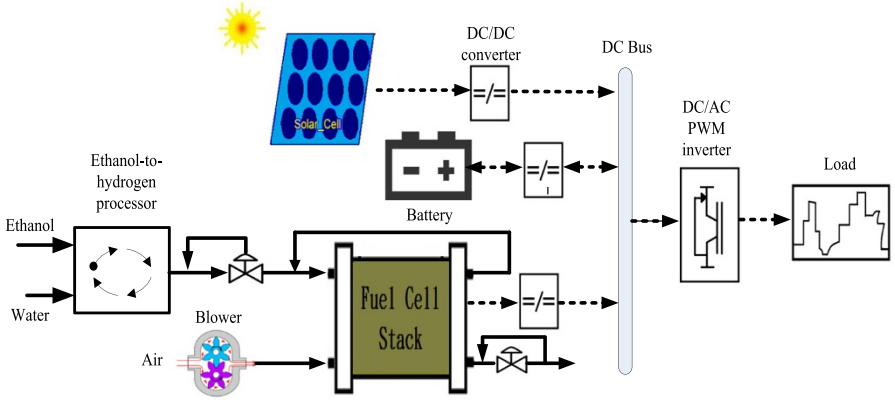

Figure 1 Hybrid power generation system.

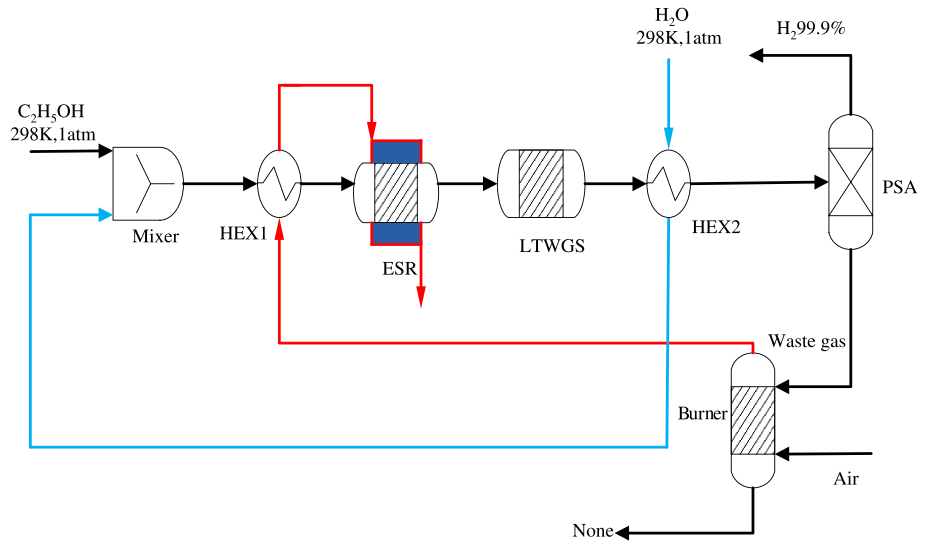

Figure 2 Stand-alone EtOH-to-H_2 processor.

Second, the kinetic models of four reactions (r_1, ..., r_4) are expressed by power-law rate expressions [12]:

$$r_1 = 2.1 \times 10^4 \exp\left(-\frac{70}{R}\left(\frac{1}{T_{ESR}} - \frac{1}{773}\right)\right) P_{C_2H_5OH} \quad (5)$$

$$r_2 = 2.0 \times 10^3 \exp\left(-\frac{130}{R}\left(\frac{1}{T_{ESR}} - \frac{1}{773}\right)\right) P_{C_2H_5OH} \quad (6)$$

$$r_3 = 1.9 \times 10^4 \exp\left(-\frac{70}{R}\left(\frac{1}{T_{ESR}} - \frac{1}{773}\right)\right) \times \left(P_{CO}P_{H_2O} - \frac{P_{C_2O}P_{H_2}}{\exp\left(\frac{4577.8}{T_{ESR}} - 4.33\right)}\right) \quad (7)$$

$$r_4 = 2.0 \times 10^5 \exp\left(-\frac{98}{R}\left(\frac{1}{T_{ESR}} - \frac{1}{773}\right)\right)\left(P_{CH_3CHO}P_{H_2O}^3\right) \quad (8)$$

where T_{ESR} is the temperature of the ESR reactor, P_i (i = C_2H_5OH, CO, H_2O, ...) is corresponding partial pressure, and R is the universal gas constant. Moreover, the one-dimensional, pseudo-homogeneous model is built by the Aspen Plus. The assumptions for the steady-state simulation of the ESR reactor include gas phase reactions, plug-flow reactor, and no pressure drop. The thermodynamic properties of some species are evaluated by using the Peng-Robinson equation of state. Other parameters include the fluid density = 0.02 kmol m^{-3}, catalyst weight = 5 kg, and sizes of the reactor with the diameter and length of the reactor D = 0.5 m and L = 1.5 m.

LTWGS reactor

To reduce CO as well as enhance hydrogen yield, the LTWGS reactor could be directly connected to the ESR reactor, where the reaction scheme is:

$$CO + H_2O \overset{Cat}{\longleftrightarrow} CO_2 + 2H_2, \quad \Delta\hat{H}_R^o = -41.15\ \text{kJ mol}^{-1} \quad (9)$$

For a moderately exothermic reaction with Sud-Chemie commercial available catalysts, we assume that the reactor is adiabatic and the operating temperature is between 400 K and 600 K. Moreover, the kinetic model is described by [13],

$$r_W = 82.2 \exp\left(-\frac{47400}{RT_{WGS}}\right)\left(P_{CO}P_{H_2O} - \frac{P_{CO_2}P_{H_2}}{K_{WGS}}\right) \quad (10)$$

where T_{WGS} is the temperature of the WGS reactor and K_{WGS} is the equilibrium constant of the WGS reaction shown by

$$\ln(K_{WGS}) = \frac{5693.5}{T_{WGS}} + 1.077\ln(T_{WGS}) + 5.44 \times 10^{-4}T_{WGS} - 1.125 \times 10^{-7}T_{WGS}^2 - \frac{49170}{T_{WGS}^2} - 13.148 \quad (11)$$

Burner

Regarding the design of burner, we assume that (i) H_2 is completely separated by PSA, (ii) all components of the burner are completely burned, and (iii) its Aspen module

is considered as an adiabatic and stoichiometric reactor. The combustion reaction in the burner is shown as follows:

$$C_2H_5OH + 3O_2 \rightarrow 2CO_2 + 3H_2O, \Delta\hat{H}^o_{b,EtOH} = -1279\ \text{kJ mol}^{-1} \quad (12)$$

$$CH_4 + 2O_2 \rightarrow CO_2 + 2H_2O, \Delta\hat{H}^o_{b,CH_4} = -803.1\ \text{kJ mol}^{-1} \quad (13)$$

$$H_2 + \frac{1}{2}O_2 \rightarrow H_2O, \Delta\hat{H}^o_{b,H_2} = -242\ \text{kJ mol}^{-1} \quad (14)$$

$$CO + \frac{1}{2}O_2 \rightarrow CO_2, \Delta\hat{H}^o_{b,CO} = -283\ \text{kJ mol}^{-1} \quad (15)$$

Sensitivity analysis

Regarding the effect of fuel utilization, the ratio of hydrogen to ethanol (H_2/C_2H_5OH) is specified by adjusting ethanol flow or water flow in the feed.

I. The profiles of H_2/C_2H_5OH vs. $(S/C)|_{H_2O}$ at different $T_{ESR,in}$ is depicted in Figure 3(a). It shows that the maximum hydrogen yield can be achieved by adjusting the water flow at constant ethanol flow. The profiles of H_2/C_2H_5OH vs. $(S/C)|_{EtOH}$ at different $T_{ESR,in}$ is depicted in Figure 3(b). Similarly, it shows that the maximum hydrogen yield is obtained by adjusting the ethanol flow at constant water flow. The corresponding operating ranges are bounded by $2 \le (S/C)|_{EtOH,H_2O} \le 2.5$ and $600K \le T_{ESR,in} \le 800K$. Notably, the manipulation of ethanol flow can ensure the larger hydrogen yield than the water flow at the same $T_{ESR,in}$, and the increase of $T_{ESR,in}$ cannot induce the high hydrogen yield. According the heat recovery design, the waste gas temperature at the outlet of heating jacket decreases when the preheated temperature of ESR increases. The low reactor temperature would reduce the conversion of ethanol reforming reactions.

II. According to the sensitivity analysis by adjusting one variable $(S/C)|_{EtOH}$, the optimization tool of Aspen Plus is employed to determine the optimal operating conditions, $(S/C)|_{EtOH} = \frac{27.2\ \text{kgmol/hr}}{12.7\ \text{kgmol/hr}} = 2.14$ at $T_{ESR,in}$ =600 K. The steady-state simulation of the system at optimal conditions is shown in Figure 4, where the flowrate of hydrogen product can achieve 55.62 kgmol/hr, i.e. H_2/C_2H_5OH =4.38 and the ethanol conversion can achieve 95%.

PEM fuel cell system

A Ballard 5 kW PEMFC stack system consists of 30 cells connected in series to provide output current up to 100 A, which is directly connected to an ethanol-to-hydrogen processor. The high purity of hydrogen produced from the processor is fed to the anode and the excess hydrogen needs to be recirculated. Referring to an empirical fuel cell stack model by [14,15], the output voltage of a single fuel cell (V_{fc}) is expressed by

$$V_{fc} = E - V_{act} - V_{ohm} \quad (16)$$

(i) The open circuit cell potential E via the Nernst equation is described by

$$E = 1.229 - 8.5 \times 10^{-4}\left(T_{fc} - 298.15\right) + \frac{RT_{fc}}{2F}\ln\left[P_{H_2}\left(P_{O_2}\right)^{0.5}\right] \quad (17)$$

(ii) The activation overvoltage V_{act} is described by a first-order dynamic with the effects of double layer capacitance charging at the electrode-electrolyte interfaces

$$\frac{dV_{act}}{dt} = \frac{i_{fc}}{C_{dl}} + \frac{i_{fc}E_{act}}{V_{act}C_{dl}} \quad (18)$$

where the activation drop E_{act} is defined by

$$E_{act} = \beta_1 + \beta_2 T_{fc} + \beta_3 T_{fc}\ln(C_{O_2}) + \beta_4 T_{fc}\ln(i_c) \quad (19)$$

and the parametric coefficients $\beta_1, \ldots, \beta_4$ are expressed by

$$\begin{aligned} \beta_1 &= -0.948 \\ \beta_2 &= 0.00286 + 0.0002\ln\left(A_{fc}\right) + 4.3 \times 10^{-5}\ln(C_{H_2}) \\ \beta_3 &= 7.6 \times 10^{-5} \\ \beta_4 &= -1.93 \times 10^{-4} \end{aligned} \quad (20)$$

and

$$\begin{aligned} C_{O_2} &= 1.97 \times 10^{-7} P_{O_2} \exp\left(\frac{498}{T_{fc}}\right) \\ C_{H_2} &= 9.174 \times 10^{-7} P_{H_2} \exp\left(\frac{-77}{T_{fc}}\right) \end{aligned} \quad (21)$$

(iii) The ohmic overvoltage is given by:

$$V_{ohm} = \frac{l_m}{A_{fc}} r_M i_{fc} \quad (22)$$

where the membrane resistivity r_M is described by

$$r_M = \frac{181.6\left[1 + 0.03\left(\frac{i_{fc}}{A_{fc}}\right) + 0.062\left(\frac{T_{fc}}{303}\right)^2\left(\frac{i_{fc}}{A_{fc}}\right)^{2.5}\right]}{\left[11.866 - 3\left(\frac{i_{fc}}{A_{fc}}\right)\right]\exp\left[4.18\left(\frac{T_{fc}-303}{T_{fc}}\right)\right]} \quad (23)$$

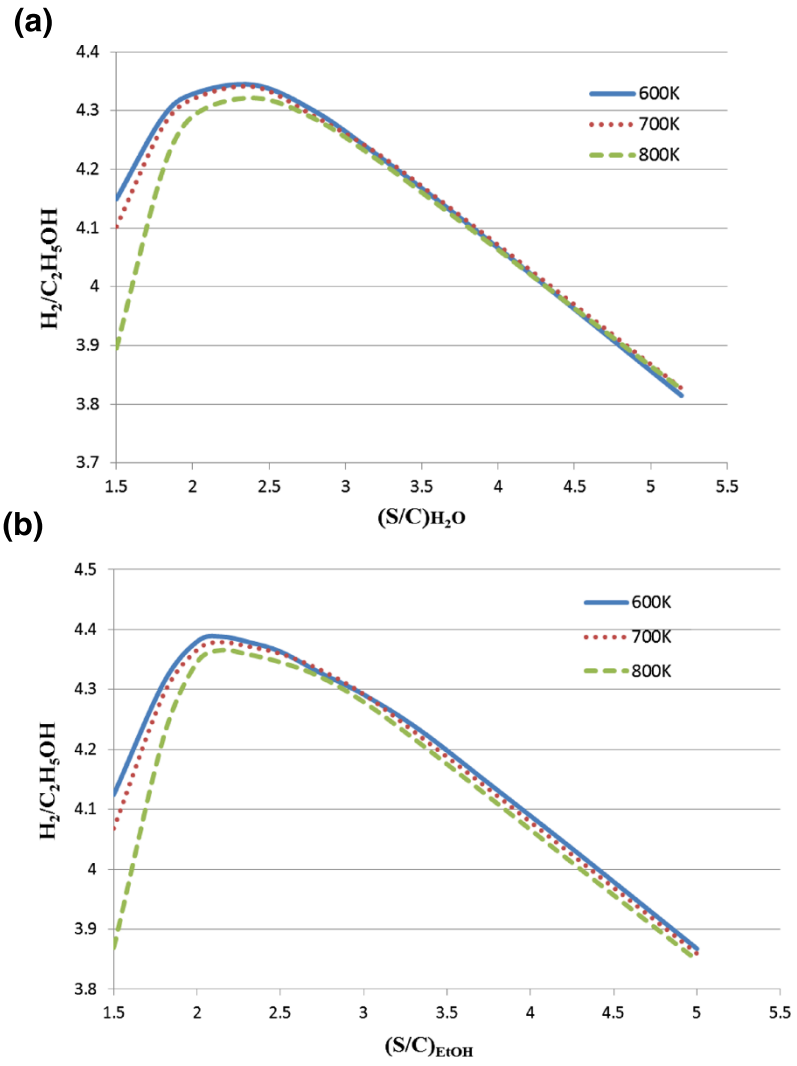

Figure 3 Fuel utilization ratio of ethanol-to hydrogen processor at different $T_{ESR,in}$ by adjusting (a) $(S/C)|_{H2O}$ (b) $(S/C)|_{EtOH}$.

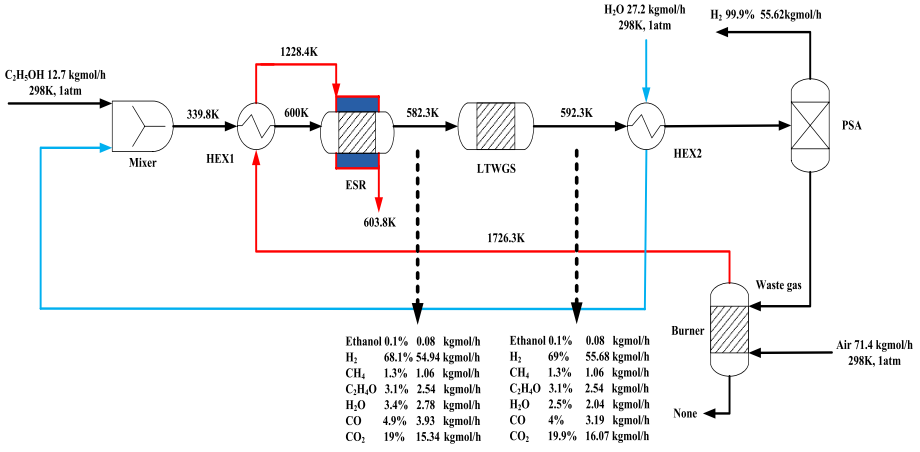

Figure 4 Optimization and simulation of EtOH-to-hydrogen processor.

Table 1 PEMFC Parameters

Parameter	Value
V_{an}	0.005 m^3
k_{an}	0.065 $mol\ s^{-1}atm^{-1}$
P_{BPR}	1 atm
V_{ca}	0.01 m^3
k_{ca}	0.065 $mol\ s^{-1}atm^{-1}$
F	96485 $Cmol^{-1}$
A_{fc}	232 cm^2
l_m	178×10^{-4} cm
R	8.314 $Jmol^{-1}K^{-1}$
C_{dl}	0.035×232 F
λ_{O_2}	2

Above of all parameters for modeling the PEMFC system have been defined in the nomenclature section. Based on the ideal gas law and the principle of mole conservation, the partial pressures of hydrogen (p_{H_2}) and oxygen (p_{O_2}) associated with reactant flow rates at the anode and cathode along with the cell current are modeled as.

$$\frac{dp_{H_2}}{dt} = \frac{RT_{fc}}{V_{an}}\left[\dot{m}_{H_2,in} - k_{an}\left(p_{H_2} - p_{H_2,in}\right) - \frac{15}{F} i_{fc}\right] \quad (24)$$

$$\frac{dp_{O_2}}{dt} = \frac{RT_{fc}}{V_{ca}}\left[\dot{m}_{O_2,in} - k_{ca}\left(p_{O_2} - p_{BPR}\right) - \frac{7.5}{F} i_{fc}\right] \quad (25)$$

Notably, two pressure regulators with fixed parameters (k_{an}, k_{ca}) are added to manipulate the outlet hydrogen flow at the anode and the outlet oxygen flow at the cathode. The above model equations show that the fuel cell performance is affected by current density (i_{fc}), fuel cell temperature (T_{fc}), hydrogen and oxygen partial pressure. Referring parameter values of the fuel cell model in Table 1, Figure 5 shows that the maximum cell power output appears when the current is operated around 250A and the cell temperature is fixed at $T_{fc} = 75$°C. Moreover, the voltage and power of the stack is given by $V_{stack} = 30V_{fc}$; $P_{fc} = V_{stack} i_{fc} A_{fc}$.

Remark 1: To address the feasible manipulation of the fuel cell stack, two pressure regulators for manipulating the outlet flow rates of hydrogen and oxygen at the anode and cathode, respectively, are required. In addition, the oxygen starvation phenomenon should be avoided, i.e., the following inequality for oxygen excess ratio (λ_{O_2}),

$$\frac{\dot{m}_{O_2,in}}{8.75 i_{fc}/F} \geq \lambda_{O_2} \quad (26)$$

should be satisfied by increasing the inlet flow rate of oxygen ($\dot{m}_{O_2,in}$) or air flow [15].

Remark 2: The stack requires a circulating water system to keep the relative humidity of membrane as well as regulate the stack temperature. It is assumed that the stack system is isothermal, the relative humidity is kept at a desired level, and the hydrogen flow in the inlet of fuel cell ($\dot{m}_{H_2,in}$). In fact, the fuel processing delays, including reaction time and transportation delay exist such that the power gap between supply and demand is inevitable.

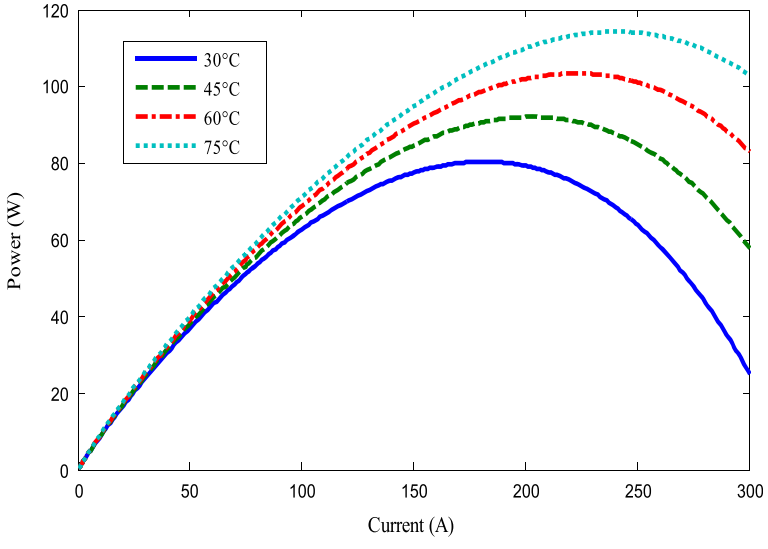

Figure 5 PEMFC power versus current at different T_{fc}.

Table 2 PV Parameters

Symbol	Value
T_0	298 K
T_{NOTC}	316 K
E_0	1000 W m^{-2}
κ	1.3854×10^{-23} J K^{-1}
E_g	1.12 eV
p_1	2.96 Am^2W^{-1}
p_2	-8.6×10^{-4} m^2W^{-1}
p_3	0.0037 K^{-1}
p_4	1272.3 AK^{-3}
R_s	1.29 Ω
R_{sh}	154.1 Ω

Photovoltaic generator

A photovoltaic (PV) generator is composed of numbers of solar cells connected in series and parallel to provide the desired output terminal voltage and current. Using the Kirchoff's current law the terminal current I_s through the solar cell is expressed by [3].

$$I_s = I_{ph} - I_d - I_{sh} \tag{27}$$

(i) The photocurrent I_{ph} is described as

$$I_{ph} = p_1 E_s \left[1 + p_2(E_s - E_0) + p_3\left(T_j - T_0\right)\right] \tag{28}$$

(ii) The diode loss current I_d is described as

$$I_d = p_4 T_j^3 \exp\left(-\frac{E_g}{\kappa T_j}\right)\left[\exp\left(\frac{e_0}{a_f N_s \kappa}\frac{V_s + R_s I_s}{T_j}\right) - 1\right] \tag{29}$$

(iii) The shunt current I_{sh} is shown by

$$I_{sh} = \frac{V_s + R_s I_s}{R_{sh}} \tag{30}$$

where the cell junction temperature T_j is expressed by

$$T_j = T_a + \frac{E_s}{800}(T_{NCOT} - 20) \tag{31}$$

where P_1, P_2, and P_3 are empirical constants. E_0 and T_0 are reference solar radiation and reference junction temperature, respectively. The P_4 is an empirical constant, a_f is the ideality factor of the PV array, E_g is the gap energy voltage of silicon, κ is Boltzmann's constant, V_s is

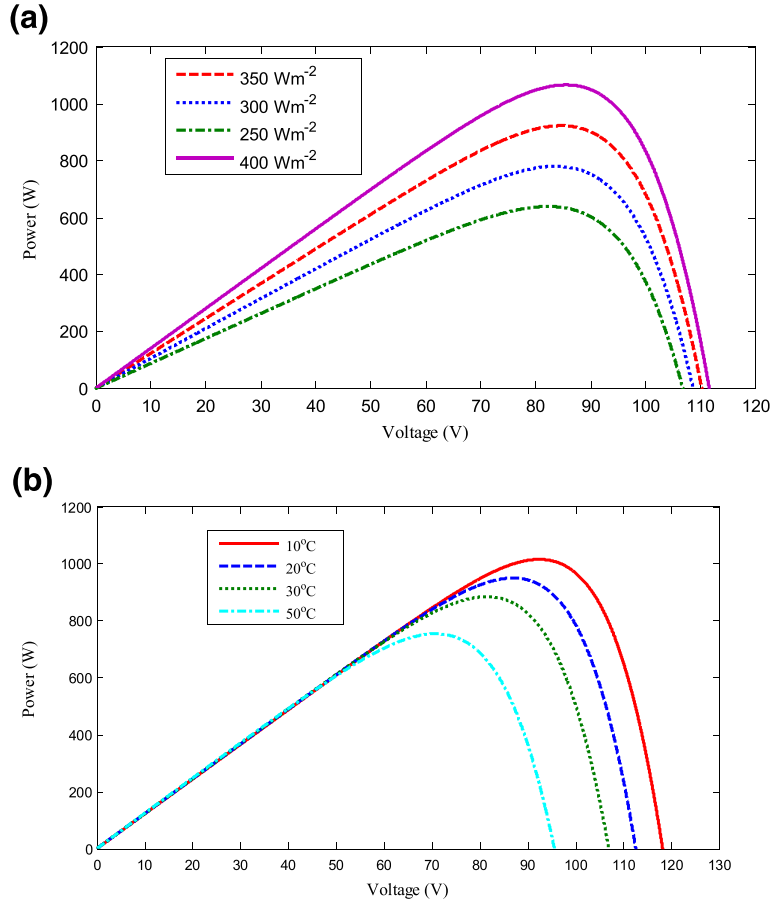

Figure 6 PV power versus voltage (a) at different E_s while $T_j = 25°C$: (b) at different T_a while $E_s = 350$ Wm^{-2}.

the terminal voltage, N_s and R_s are the number of cells in series and series resistance, and R_{sh} is the parallel resistance. All the above parameter values for the PV system are shown in Table 2. Figure 6 shows that the maximum power output of the PV system exists at different T_a and E_s.

Auxiliary devices

The auxiliary devices shown in Figure 1 include a lithium-ion battery which is considered as a high-capacity energy storage to compensate the power gap and share the load demand and several he boost DC/DC converters are used to boost the DC voltage of the units of PV, PEMFC and battery. The dynamic responses of battery are faster than other units in the hybrid power system, in our approach the modeling of battery is omitted and the well-defined charging/discharging mechanism is considered [16,17]. The DC/AC pulse-width modulation (PWM) is used to meet the specification of the household electricity, where the dynamics with regard to AC voltage and current waveform are shown in Figure 7 using the SimPowerSystems™ toolbox in Matlab.

Scenario analysis

For the proposed HPG system, the solar irradiance, water and ethanol are denoted as energy sources. Assumed that the weather variation is inevitable and the sources of water and ethanol are reliable, the HPG system is considered as the optimal power generator since the optimized EFC power generator according to optimal operating conditions in Figures 4 and 5 is specified and the maximum PV power in Figure 6 is achieved by using the maximum power point tracking (MPPT) controller. Moreover, scenario analysis of the daily operation of the HPG system is addressed as follows.

1. *Hybrid power dispatch*: Figure 8(a) shows that the PV and PEMFC systems are dispatched to precisely meet the daily household load demand [3]. In our design, the daily PV power distribution shown in Figure 8(b) is fixed according to prescribed patterns of solar irradiance. A scenario shows that both PV and PEMFC are integrated to instantly cope with the peak power. Especially, the EFC power should dominate the main electricity supply during the day and night.
2. *Power gap compensation*: If the EtOH-to-H_2 processor cannot produce pure hydrogen immediately due to slow reactions, then the EFC power decay at this moment. It is caused by the fuel processing delay such that the power demand gap (desired P_{fc}-actual P_{fc}) shown in Figure 8(b) appears. Assumed that the rapid response of Li-ion battery can instantly compensate the power demand gap and the battery charging from PV and EFC units is always larger than the battery

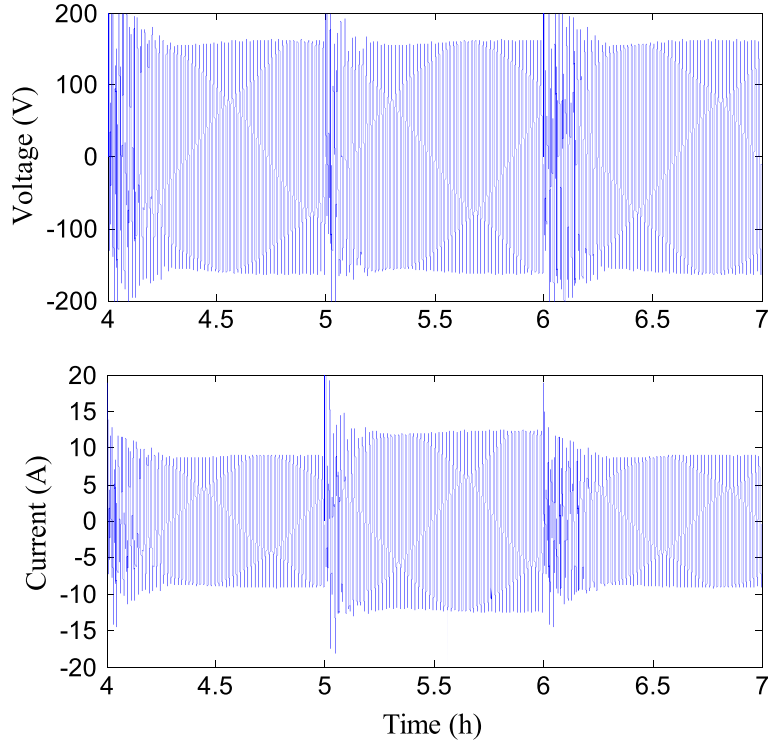

Figure 7 DC/AC PWM inverter connected to DC/DC converter.

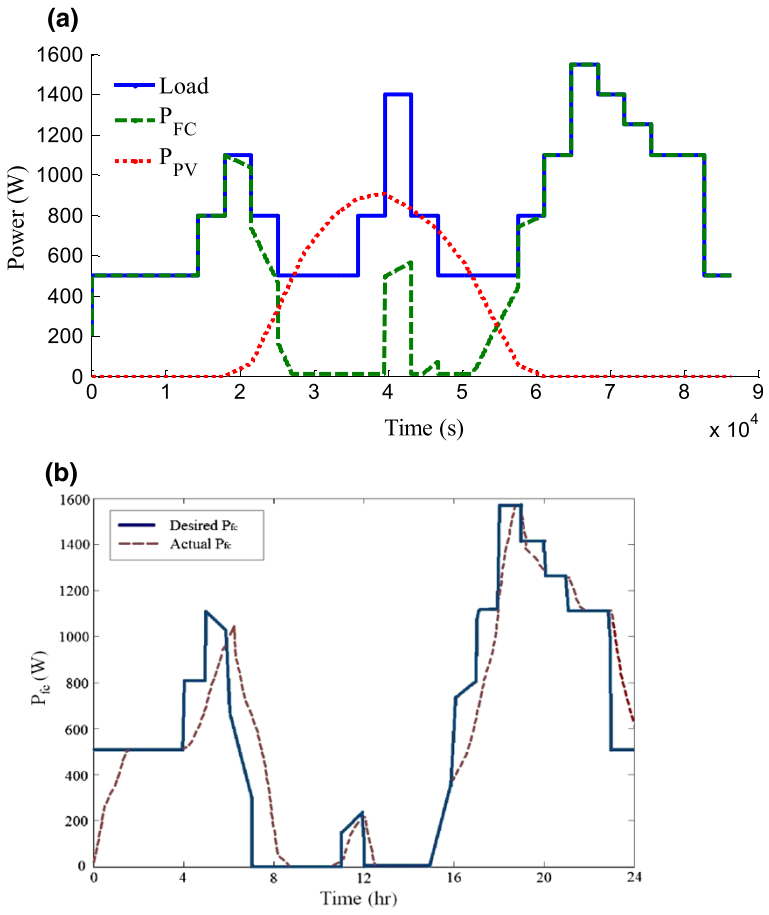

Figure 8 The daily operation of HPG system without use of battery: (a) Power profiles from P_{FC} and P_{PV}; (b) Responses of EFC power generator.

discharging, Figure 9(a) and 9(b) show that the HPG system can precisely meet the daily load demand. In this perfect scenario, the hybrid power dispatching shown in Figure 9(a) is confirmed where the battery contribution (green area) aims to compensate the power demand gap during each time period. Figure 9 (b) shows that the battery is recharged by the excess power from PV and PEMFC during day and night.

Regarding hybrid power dispatching problem, the PV unit (blue bars) provides 34.5% total power, the battery (green bars) is 12.4% and the EFC (red bars) is about 53.1%. Notably, the battery is charged from the EFC is about 56.1% and 43.9% from the PV. It implies that the PV power is used to save 39.9% fuel consumption.

System efficiency

The efficiency of the power generation system is usually affected by the electric power, mechanical energy and heat. To ignore the effects of mechanical energy and heat, the efficiency of the HPG system is investigated as follows.

A. Photovoltaic efficiency

According to the formulation of solar cell efficiency limits [18], the PV efficiency is described as

$$\eta_{\max} = \frac{P_{\max}}{E_s A_s} \tag{32}$$

where $\eta_{\max}$ is the maximum efficiency of the PV system, $P_{\max}$ is the maximum PV power, and A_s is the surface area of the solar panel.

B. EFC efficiency

Referring the experimental data for ethanol reforming processes [19,20], the energy efficiency of EtOH-to-H_2 processor is defined as

$$\eta_{ESR} = \frac{\dot{m}_{H_2,in}\mathrm{HHV}_{\mathrm{H_2}}}{\dot{m}_{EtOH,in}\mathrm{HHV}_{\mathrm{EtOH}} + \dot{m}_{\mathrm{H_2O},in}\mathrm{HHV}_{\mathrm{H_2O}}} \tag{33}$$

and the energy efficiency of fuel cell is described as

$$\eta_{fc} = \frac{P_{fc}}{\dot{m}_{H_2,in}\mathrm{HHV}_{\mathrm{H_2}}} \tag{34}$$

where HHV_i represent the high heating value of species i. $\dot{m}_{EtOH,in}$ and $\dot{m}_{H_2O,in}$ represent the inlet flow rate of

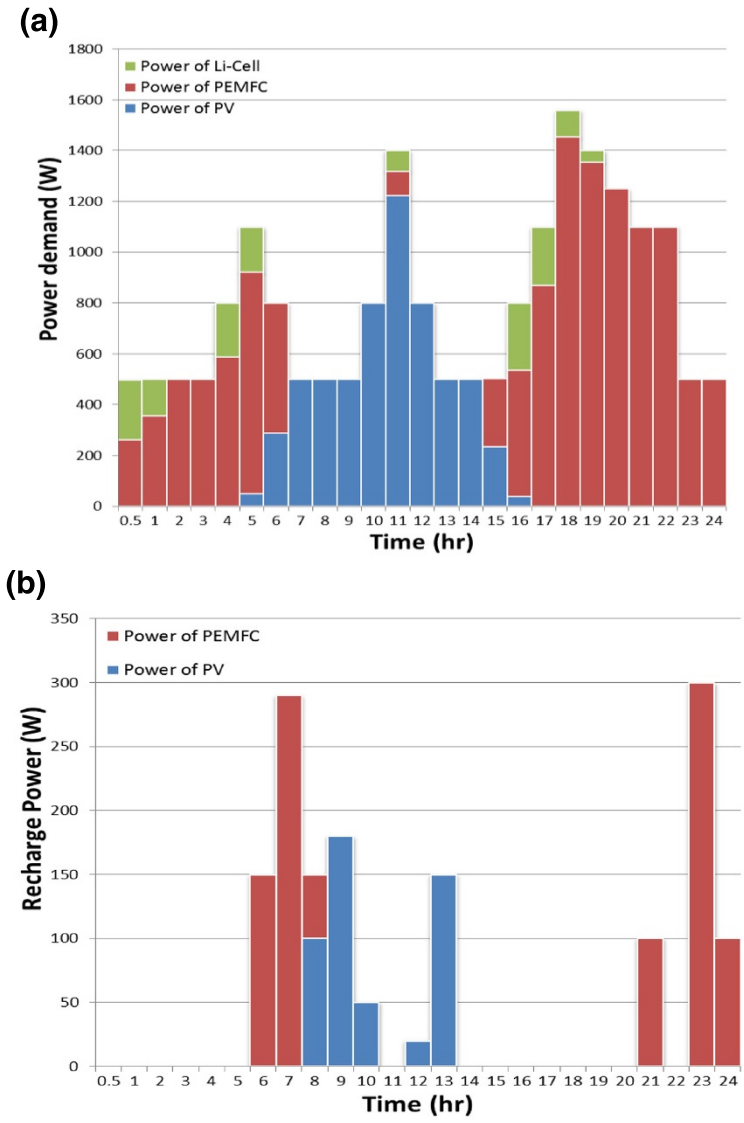

Figure 9 HPG system according to daily power demand: (a) Hybrid power dispatch; (b) Recharge power for battery.

ethanol and water, respectively. Moreover, the efficiency of the EFC is expressed by $\eta_{efc} = \eta_{esr}\eta_{fc}$. Figure 10 shows that the energy efficiency of the EFC unit is increasing if the load demand increases, but the energy efficiency of the FC unit without the use of EtOH-to-H_2 processor decreases if the load demand is larger than 5 kW. It is verified that the EFC design can ensure higher energy efficiency than the conventional hydrogen fueled fuel cell system.

C. According to above efficiency of each unit, the (overall) system efficiency of HPG system is expressed as

$$\eta_{overall} = \frac{(P_{PV} + P_{fc} + P_{battery})\eta_{converter}\eta_{inverter}}{P_{PV}/\eta_{\max} + P_{fc}/\eta_{efc} + P_{battery}/\eta_{battery}} \quad (35)$$

where $\eta_{battery}$, $\eta_{converter}$ and $\eta_{inverter}$ are efficiencies of Li-ion battery, DC/DC converter and DC/AC inverter, respectively. The battery power $P_{battery}$ is evaluated by $P_d - P_{efc} - P_{PV}$ where P_d is set as the load. Referring the initial efficiency of Li-ion battery [21], we assume $\eta_{battery}$ for a new battery. Referring to references [22,23], we assume $\eta_{converter}$ =0.9 and $\eta_{inverter}$ = 0.98. Referring the hybrid power dispatching in Figure 9(a), the hybrid system efficiency by Eq. (35) is shown in Figure 11. Based on the hybrid power system using parallel and series connections, the system efficiency is around 11% during the day, but it reaches over 60% during the night. Obviously, the PV system induces lower system efficiency and it can be significantly improved by using the integrated reformer/fuel cell system and battery.

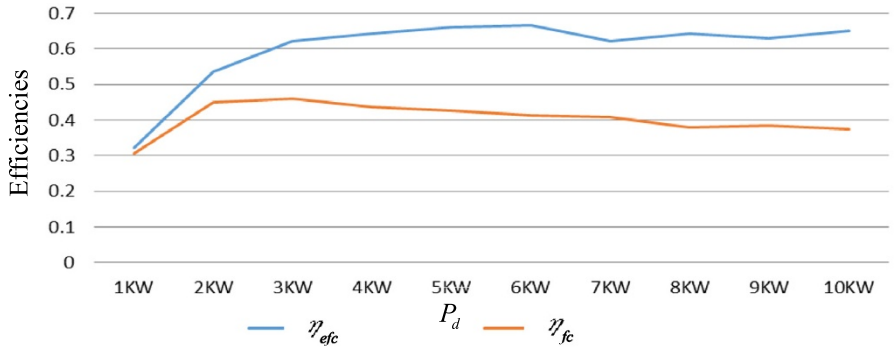

Figure 10 Energy efficiencies for EFC and PEMFC.

Conclusions

An optimized fuel processing unit using ethanol fuel can produce high-purity hydrogen. The simulation shows that the stand-alone EtOH-to-H2 processor not only guarantee higher energy efficiency, but also it can continuously produce hydrogen if the fuel is enough. According to scenarios for the daily operation of the HPG system, the EFC power dominates the power supply during the night, the PV system dominates the power supply during the day and the backup battery aims to instantly compensate the power gap and store the excess power from PV or EFC. According to the hybrid power dispatch, the distribution of the HPG system efficiency is specified.

Nomenclature

a_f, ideality factor
A_{fc}, effective fuel cell area, cm^2
A_s, surface area of the solar panel, m^2
C_{O_2}, oxygen concentration at the cathode/membrane interface, $molm^{-3}$
C_{H_2}, hydrogen concentration at the anode/membrane interface, $molm^{-3}$
C_{dl}, Double layer capacitance, F
E_0, Reference solar radiation, $W\ m^{-2}$
E_g, Gap energy voltage for silicon, eV
E_s, solar radiation, Wm^{-2}
i, current density, Acm^{-2}
I_s, terminal current of PV cell, A
k_{an}, k_{ca}, flow constant of anode and cathode, $mol\ s^{-1}atm^{-1}$
l_m, Membrane thickness, cm
c_p, specific heat capacity, $J\ K^{-1}kg^{-1}$
P_i, partial pressure of i component, atm
P_{BPR}, back pressure, atm
P, cell power, W
T_a, ambient temperature, K
T_0, reference junction temperature, K
T_{NCOT}, normal cell operating temperature, K
R_s, series resistance, Ω
R_{sh}, parallel resistance, Ω
u, superficial velocity, $m\ s^{-1}$
V_s, terminal voltage of PV cell, V

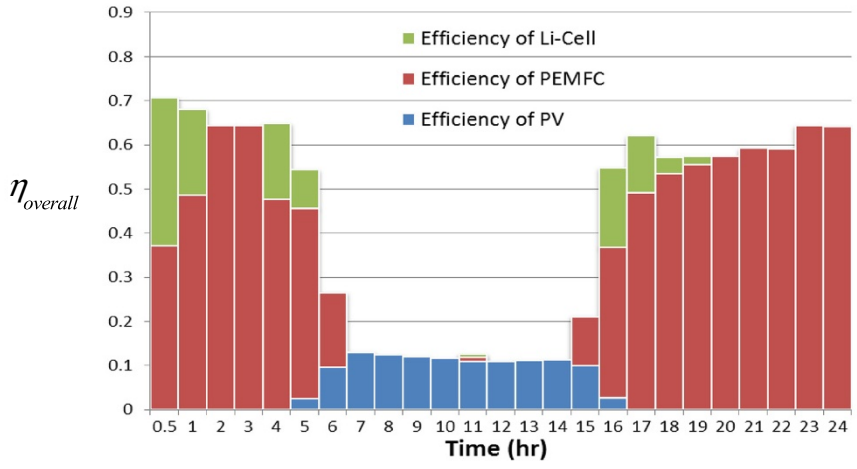

Figure 11 HPG system efficiency.

Competing interests
The authors declare no competing financial interests.

Authors' contributions
The energy efficiency of the ethanol-fueled fuel cell (EFC) is higher than the hydrogen-fueled fuel cell system. With the aid of the stand-alone EtOH-to-H2 processor and backup battery. The HPG system efficiency according to hybrid power dispatch is improved. All authors read and approved the final manuscript.

Acknowledgment
The authors would like to thank the National Science Council of the Republic of China for financially supporting this research under Contract No. NSC 100-2211-E-006-264.

Author details
[1]Department of Chemical Engineering, National Cheng Kung University, Tainan 70101, Taiwan. [2]National Yunlin University of Science and Technology, Douliou, Yunlin 64002, Taiwan.

Received: 27 November 2013 Accepted: 14 February 2014
Published: 4 March 2014

References

1. Muselli M, Notton G, Louche A: **Design of hybrid-photovoltaic power generator, with optimization of energy management.** *Sol Energy* 1999, **65:**143–157.
2. Elhadidy MA: **Performance evaluation of hybrid (wind/solar/diesel) power systems.** *Renew Energy* 2002, **26:**401–413.
3. Hwang JJ, Lai LK, Wu W, Chang WE: **Dynamic modeling of a photovoltaic hydrogen fuel cell hybrid system.** *Int J Hydrogen Energy* 2009, **34:**9531–9542.
4. Uzunoglu M, Onar OC, Alam MS: **Modeling, control and simulation of a PV/FC/UC based hybrid power generation system for stand-alone applications.** *Renew Energy* 2009, **34:**509–520.
5. Zervas PL, Sarimveis H, Palyvos JA, Markatos NCG: **Model-based optimal control of a hybrid power generation system consisting of photovoltaic arrays and fuel cells.** *J Power Sources* 2008, **181:**327–338.
6. Yilanci A, Dincer I, Ozturk HK: **A review on solar-hydrogen/fuel cell hybrid energy systems for stationary applications.** *Prog Energy Combust Sci* 2009, **35:**231–244.
7. Gupta RB: *Hydrogen Fuel: Production, Transport, and Storage.* USA: CPC press; 2009.
8. Shekhawat D, Spivey JJ, Berry DA: *Fuel Cells: Technologies for Fuel Processing.* UK: Elsevier; 2007.
9. Wu W, Tungpanututh C, Yang HT: **A conceptual design of a stand-alone hydrogen production system with low carbon dioxide emissions.** *Int J Hydrogen Energy* 2012, **37:**10145–10155.
10. Garcia VM, Lopez E, Serra M, Llorca J: **Dynamic modeling of a three-stage low-temperature ethanol reformer for fuel cell application.** *J Power Sources* 2009, **192:**208–215.
11. Degliuomini LN, Biset S, Luppi P, Basualdo MS: **A rigorous computational model for hydrogen production from bio-ethanol to feed a fuel cell stack.** *Int J Hydrogen Energy* 2012, **37:**3108–3129.
12. Uriza I, Arzamendi G, Lopez E, Llorca J, Gandia LM: **Computational fluid dynamics simulation of ethanol steam reforming in catalytic wall microchannel.** *Chem Eng J* 2011, **167:**603–609.
13. Choi Y, Stenger HG: **Water gas shift reaction kinetics and reactor modeling for fuel cell grade hydrogen.** *J Power Sources* 2003, **124:**432–439.
14. Khan MJ, Iqbal MT: **Analysis of a small wind-hydrogen stand-alone hybrid energy system.** *Appl Energy* 2009, **86:**2429–2442.
15. Wu W, Xu JP, Hwang JJ: **Multi-loop nonlinear predictive control scheme for a simplistic hybrid energy system.** *Int J Hydrogen Energy* 2009, **34:**3953–3964.
16. Knauff M, McLaughlin J, Dafis C: *Simulink model of a lithium-ion battery for the hybrid power system test-bed*, ASNE Intelligent Ships Symposium, Philadelphia, PA, USA; 2007.
17. Erdinc O, Vural B, Uzunoglu M: *A dynamic lithium-ion battery model considering the effects of temperature and capacity fading*, 2nd International Conference on Clean Electrical Power, Capri, Italy; 2009.
18. Nelson J: *The Physics of Solar Cell.* UK: Imperial College Press; 2003.
19. Deluga GA, Salge JR, Schmidt LD, Verykios XE: **Renewable hydrogen from ethanol by autothermal reforming.** *Science* 2004, **303:**933–937.
20. Hung CC, Chen SL, Liao YK, Chen CH, Wang JH: **Oxidative steam reforming of ethanol for hydrogen production on M/Al2O3.** *Int J Hydrogen Energy* 2012, **37:**4955–4966.
21. Shen J, Tang Y, Liang Y, Tan X: **Relationship between initial efficiency and structure parameters of carbon anode material for Li-ion battery.** *J Cent South Univ Technol* 2008, **15:**484–487.
22. Ma D, Ki WH, Tsui CY, Mok PKT: *A single inductor dual-output integrated dc/dc boost converter for variable voltage scheduling*, Proceeding of the ASP-DAC, Asia and South Pacific; 2001.
23. Anis RA: **Stepped sine wave DC/AC inverter I. Theoretical analysis.** *Energy Mater Sol Cells* 1992, **28:**123–130.

doi:10.1186/2043-7129-2-5
Cite this article as: Wu *et al.*: Scenario analysis of a bioethanol fueled hybrid power generation system. *Sustainable Chemical Processes* 2014 **2**:5.